Model for carrier dynamics and photoluminescence quenching in wet and dry porous silicon thin films

Louis Brus
AT&T Bell Labs, Murray Hill, New Jersey 07974
(Received 31 July 1995; revised manuscript received 21 September 1995)

A simple model of electron kinetics, previously used in molecular and protein electron dynamics, is applied to transport and photoluminescence in wet and dry porous Si. Porous Si is modeled as a system of touching Si nanocrystals that individually show strong three-dimensional confinement. In the presence of a polar liquid in the pore structure, the electron-polar molecule dynamical coupling is an order of magnitude stronger than the electron-Si acoustical-phonon coupling. Dry porous Si shows resonant tunneling kinetics, while wet porous Si shows fast, activationless, highly exothermic transfer typically characteristic of protein systems. The calculations explain why photoluminescence is strong in dry porous Si, while conductivity and electroluminescence are enhanced in wet porous Si. It is suggested that hot carrier relaxation rates in Si nanostructures would be faster in a polar environment.

I. INTRODUCTION

Porous silicon (p-Si), made by hydrogen fluoride electrochemical etching of crystalline wafer Si, typically is a rather open, microns-thick thin film composed of touching Si particles, and/or randomly interconnected Si ''wires'' of variable, undulating diameter.[1] In samples of ~80% porosity, characteristic dimensions are 1–10 nm. In dry p-Si films, visible red photoluminescence is observed with 10^{-3}–10^{-5} s lifetime, and typically a few percent quantum yield at room temperature. The emission is generally attributed to nanocrystals, and locally wider sections of the wires that can be thought of as Si nanocrystals partially fused to their neighbors. These Si nanocrystals have band gaps near 2.0 eV because of quantum confinement. Quite similar red luminescence occurs in Si nanocrystals made by aerosol methods.[2] The nanocrystal photoluminescence quantum yield greatly increases over that of bulk crystalline Si because the nonradiative Auger and trapping processes that quench emission in wafer Si are effectively decreased in nanocrystalline Si.[3]

p-Si electrical transport and luminescence properties are very sensitive to the presence of a polar liquid, and even its dilute vapor, inside the internal pores. Conductivity increases by orders of magnitude,[4] red photoluminescence is quenched,[5] and electroluminescence improves dramatically.[6] These changes are reversible and must have some physical rather than chemical origin. Methanol and water do not have electron donor or acceptor energy levels inside Si crystallite band gaps, and thus cannot directly exchange carriers with Si nanostructures. In this paper, I develop a simple model, previously employed in protein and molecular electron transfer dynamics, for the role of polar liquids in carrier *dynamics* to explain these observations. Polar liquids increase the rates of nonresonant electron transfer processes through direct ''electron-polar molecule'' coupling.

Section II reviews Si nanocrystal energy levels as a function of size. Section III outlines the model, and Sec. IV applies it to several specific problems. Section V analyzes the p-Si data, and discusses other possible implications of direct carrier-polar molecule coupling in nanostructures.

II. ELECTROSTATICS

Electrostatic polarization is important in the energetics of isolated nanocrystals and p-Si.[7,8] The fact that the Coulomb energy is screened in bulk semiconductors ($\epsilon_{Si}=11$) necessarily implies that carriers in nanocrystals have size-dependent dielectric polarization energies. The classical electrostatic energy $P(r)$ of an electron at radius r in a spherical Si nanocrystal of diameter d, in silicon dioxide host as an example, is shown in Fig. 1. $P(r)$ is

$$P(r)=\frac{e^2}{d}\sum_n [(\epsilon-1)(n+1)/\epsilon(\epsilon_{Si}n+n+1)](2r/d)^{2n}, \tag{1}$$

where $\epsilon=\epsilon_{Si}/\epsilon_{oxide}$. There is an image force pulling the charge to the crystallite center, which is the point of greatest

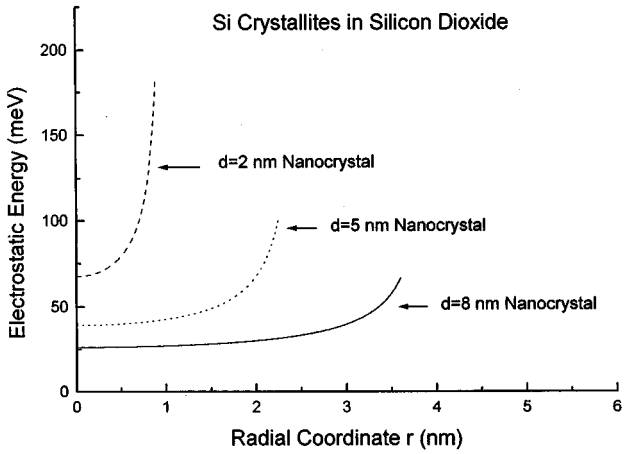

FIG. 1. Equation (1) electrostatic potential energy for one excess carrier in a Si nanocrystal in silicon dioxide. Zero energy is the conduction-band edge (or valence-band edge) in bulk Si.

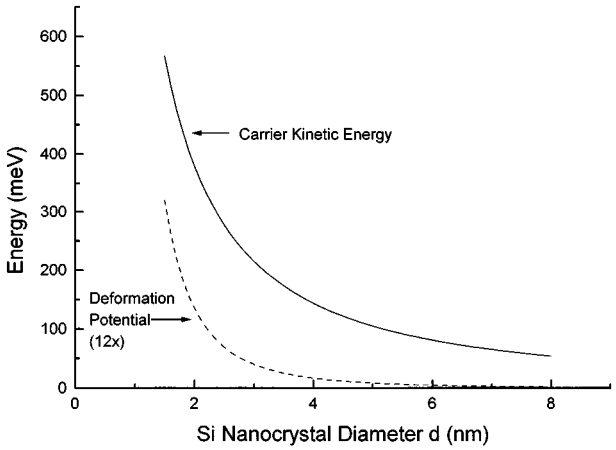

FIG. 2. Upper trace: Carrier kinetic energy (averaged between hole and electron) adapted from Ref. 10(d). Lower trace: size-dependent deformation potential reorganization energy as described in the text.

dielectric stabilization, because $\epsilon_{Si}=11$ and $\epsilon_{oxide}=3.75$. The center potential is shifted up from the bulk Si conduction-band edge, by about 40 meV in 5-nm nanocrystals, as there is less polarization energy stored in the SiO_2 than would be in bulk Si host.

The Si static dielectric constant decreases in nanocrystals as quantum confinement changes the optical absorption spectrum.[9] The effective dielectric constant becomes a function of d. If this is taken into account, then Lannoo and co-workers have shown that Eq. (1) accurately represents the potential acting on an electron in a Si nanocrystal[8(d)] in vacuum. ϵ_{Si} decreases from 11 in bulk Si to 6.5 for $d=2$ nm.

The lowest eigenvalue of $P(r)$ with the size-dependent ϵ_{Si} in Schrödinger's equation for the extra electron gives the size dependence of the single nanocrystal electron affinity.[7,8] The electron affinity decreases as size decreases. It is important to obtain the correct quantitative ratio between the kinetic and potential energy terms. Simple parabolic band, effective-mass models with kinetic energy $\propto d^{-2}$ significantly overestimate the kinetic energies in Si nanocrystals, as judged by the predicted band-gap dependence upon size.[10] For this calculation, I adopt the Hill and Whalley[10] kinetic energy KE(d) in Fig. 2, which scales approximately as $d^{-1.4}$, and which reproduces the experimental band gaps of Si nanocrystals if the Coulomb interaction is additionally included.[10(d),10(e)] While the hole kinetic energy in Si is larger than the electron energy, I use an average of the two to represent a generic ''carrier'' in the hopping calculations. (In Si the actual electron wave function is valley-orbit degenerate, and is strongly anisotropic if just one valley is involved. At 23 C the wave function should fluctuate among the degenerate valleys in one nanocrystal, and on average will have a symmetric $1S$-type charge distribution.)

In a nanocrystal with a $1S$ charge distribution, the electron affinity decreases by an amount ΔA from the 4.5-eV value of bulk Si (i.e., the energy of the conduction-band edge below the electron in vacuum reference),[7,8(d)]

$$\Delta A = \mathrm{KE}(d) + \langle 1S|P(r)|1S\rangle, \tag{2}$$

where

$$\langle 1S|P(r)|1S\rangle \simeq (e^2/d)(1/\epsilon_{out} - 1/\epsilon_{Si}) + \delta\Sigma. \tag{3}$$

The first term above is the $n=0$ term in the average of $P(r)$ over $1S$. ϵ_{out} refers to the medium outside the nanocrystal. $\delta\Sigma$ contains the $n>0$ terms and can be approximated as[8(d)]

$$\delta\Sigma = \frac{0.94e^2}{\epsilon_{Si}d}\left(\frac{\epsilon_{out}-\epsilon_{Si}}{\epsilon_{out}+\epsilon_{Si}}\right). \tag{4}$$

In vacuum, $\delta\Sigma$ is about 8% of the $n=0$ term, while in water the two terms are of the same magnitude.

III. ELECTRON KINETICS

Consider an extra electron on a nanocrystal of diameter d_1 hopping to a second, touching, and neutral nanocrystal with diameter d_2. The electron's field exits the nanocrystal and terminates at infinity. The transfer free-energy difference ΔG_t is

$$\Delta G_t = \Delta A(d_2) - \Delta A(d_1). \tag{5}$$

Here, I neglect a small charge-induced dipole term caused by the proximity of the two spheres, and a small acoustical phonon energy to be discussed in detail below. If $d_2>d_1$, $\Delta G<0$; this exothermicity is $\sim$500 meV for transfer from a 2- to a 4-nm nanocrystal in vacuum, for example. In red emitting Si nanocrystals with band gaps near 2.0 eV, the electronic levels are strongly quantized in three dimensions, and therefore discrete. To transfer into the ground $1S$ state of the larger nanocrystal, the electron must dissipate the exothermicity in coupled ''vibrational'' degrees of freedom.

In covalent Si, electrons are weakly coupled to acoustic phonons by the deformation potential. In nanocrystals, and more generally in localized semiconductor states of all types, deformation coupling increases roughly as d^{-3}.[11] This coupling $\lambda_{dp}(d)$ is the vertical Franck-Condon energy between the phonon harmonic potential with the electron on the nanocrystal, and the shifted potential for the neutral nanocrystal. A somewhat similar deformation potential coupling, increasing in smaller nanocrystals, exists when the nanocrystal contains both an electron and a hole. This ''band gap'' deformation potential shift has been estimated by Lannoo and co-workers[12] for Si nanocrystals. As an approximation, I take $\lambda_{dp}(d)$ in Fig. 2 to be one-half the ''band-gap'' deformation potential. For a 2-nm nanocrystal, λ_{dp} is only $\sim$12 meV; this approximation is probably good to a factor of two.

The simple theory of electron transfer from a localized state, arbitrarily strongly coupled to a vibrational mode, has developed independently in the solid state and chemical dynamics communities. In both cases a diabatic two-state model, linearly coupled to a heat bath, is invoked, and similar final equations are obtained. Holstein, Henry and Lang, and Ridley originally developed the theory for deep traps and small polarons in semiconductors.[13] Delerue and Lannoo extended this theory to calculate trapping rates onto surface states, in Si nanocrystals embedded in SiO_2.[8(c),14] In chemical dynamics, Marcus and others developed the theory for electron transfer involving molecules and proteins, in liquids and in biological membranes.[15] In chemical dynamics models, a polar solvent is directly incorporated.

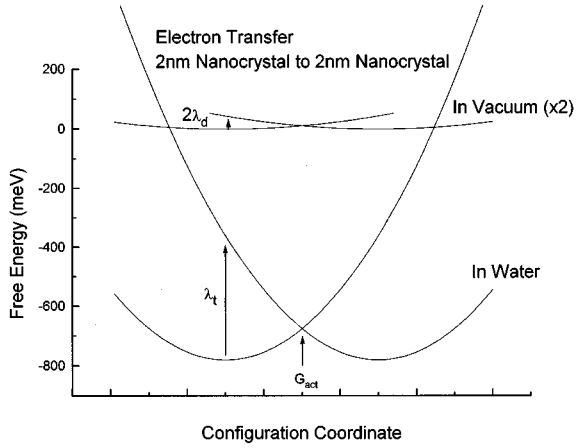

FIG. 3. Free-energy configuration coordinate diagram for electron transfer from a 2-nm nanocrystal to another 2-nm nanocrystal. Upper trace: transfer in vacuum for electron coupled by deformation potential to Si acoustical modes. Lower trace: transfer in water for electron coupled to both Si acoustical modes and water. Zero of energy is the energy of an excess electron in a 2-nm nanocrystal in vacuum.

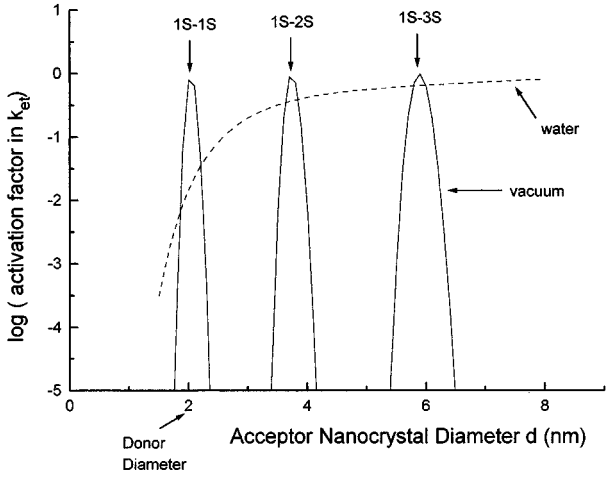

FIG. 4. Logarithmic plot (base 10) of Eq. (3) activation factor in the transfer rate at 23 C, for transfer from a 2-nm donor nanocrystal to acceptor nanocrystals of varying diameter. $1S$-$2S$ refers to the donor state $1S$ and acceptor state $2S$, etc. Zero on the vertical axis corresponds to zero activation energy $G_{\rm act}$.

In all these models the coupled vibrational degree of freedom creates a kinetic barrier. At low temperature electron transfer may involve nuclear tunneling, but at high temperature the rate is controlled by thermal activation over a barrier $G_{\rm act}$. Figure 3 is a symmetric vibrational configuration coordinate diagram for electron transfer when $d_1=d_2$. The vertical energy $2\lambda_{\rm dp}$ is the acoustical reorganization energy necessary for the electron to transfer from 1 to 2. It is the sum of the Franck-Condon shifts in both nanocrystals. The vibrational activation energy $G_{\rm act}$ is $\lambda_{\rm dp}/2$ in this symmetric case where $\Delta G=0$.

In general, the high-temperature limit of the unimolecular transfer rate has the form[13(b),15(e)]

$$k_{\rm et}(s^{-1})=(4\pi^2/h)H_{\rm rp}^2(4\pi\lambda k_BT)^{-1/2}\exp\{-G_{\rm act}/k_BT\}, \tag{6}$$

where

$$G_{\rm act}=(\lambda+\Delta G)^2/4\lambda. \tag{7}$$

Here T is absolute temperature, λ is the total reorganization energy, k_B is Boltzmann's constant, h is Planck's constant, and $H_{\rm rp}$ is the electronic coupling element between initial and final diabatic states. When $G_{\rm act}$ is large, $k_{\rm et}$ decreases by many orders of magnitude. For fast, activationless transfer, λ must equal $-\Delta G$.

In such models, electronic energies, both fast and slow dielectric polarization energies, and phonon Franck-Condon energies, all contribute to ΔG. Only slow polarization energies and the phonon Franck-Condon energies contribute to λ. If the transfer were exactly resonant, and the electron not coupled to phonons or a polar fluid, then the transfer time would be on the order of $h/H_{\rm rp}$.

IV. MODEL CALCULATIONS

A. Electron transport between nanocrystals

In Si, $\lambda_{\rm dp}$ is small. Figure 4 is a logarithmic plot of the exponential activation factor in $k_{\rm et}$, for 23-C electron transfer between touching nanocrystals. The initially charged donor size is 2 nm, and ΔG_t is given by Eq. (5). On resonance the transfer is nearly activationless when $d_1=d_2$. However, off resonance $k_{\rm et}$ quickly decreases because of the small deformation potential coupling. The width of the resonance is proportional to $\lambda_{\rm dp}$.

In transfer to larger nanocrystals, direct hopping to the $1S$ state is negligible because of large ΔG_t. However, nearly resonant transfer to excited discrete acceptor states such as $2S$ and $3S$ will occur.[16] I assume that the $2S$ and $3S$ energies scale as $3\mathrm{KE}(d_2)$ and $8\mathrm{KE}(d_2)$, as occurs for simple quantum confinement of an electron in a sphere. Figure 4 shows that $1S$-$2S$ transfer becomes resonant at $d_2=3.8$ nm, and $1S$-$3S$ at $d_2=6.0$ nm.

If there is a polar fluid outside the nanocrystals, there will be long-range electrostatic coupling to the liquid motions, as well as short-range coupling to Si acoustical modes. Electrostatic reorganization energy in this geometry—two touching spherical cavities in water—has been previously analyzed for proteins and molecules in aqueous environments, in the limit where the liquid is a polarizable continuum.[15(a)] The total reorganization energy accompanying electron transfer for touching nanocrystals becomes $\lambda_t=2\lambda_{\rm dp}+\lambda_{\rm out}$ where

$$\lambda_{\rm out}=e^2\{1/d_1+1/d_2-1/d_{12}\}(1/\epsilon_{\rm op}-1/\epsilon_s), \tag{8}$$

and $d_{12}=d_1+d_2$. $\epsilon_{\rm op}$ and ϵ_s are the fluid optical and static dielectric constants. For water, $\epsilon_s=80$ and $\epsilon_{\rm op}=1.75$. Physically, the water is initially polarized around the charged nanocrystal. When the charge transfers, this orientation must relax, and an equivalent orientation forms around the acceptor nanocrystal. The response time of the water is slow with respect to electron motion, and thus a barrier is created in the Franck-Condon sense. The electric field at the surface of a singly charged, 3-nm nanocrystal is on the order of 5×10^6 V/cm—a value not large enough to significantly saturate ϵ_s.[17]

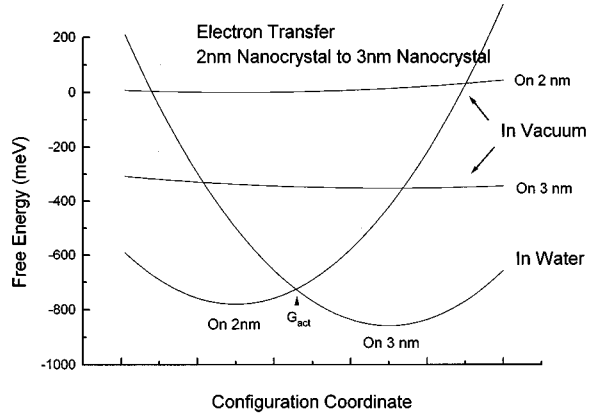

FIG. 5. Similar plot to Fig. 3, in this case for transfer from a 2-nm nanocrystal to a 3-nm nanocrystal.

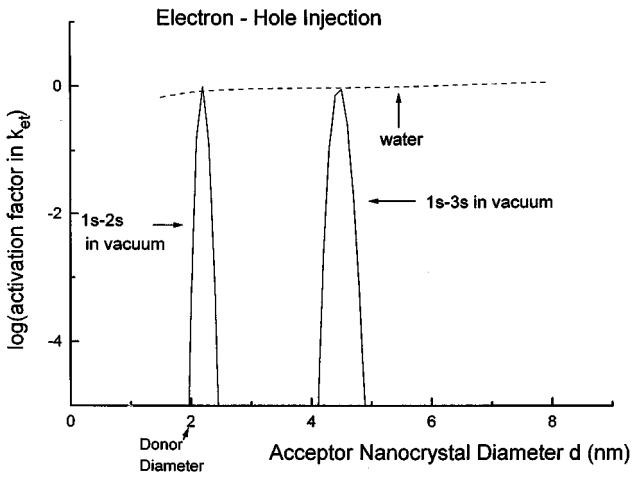

FIG. 6. Similar plot to Fig. 4, in this case for transfer of one carrier in a 2-nm donor nanocrystal into an acceptor nanocrystal already containing the opposite sign carrier.

This classical model of incorporating solvent polarization through harmonic free-energy surfaces, proposed some 40 years ago, has recently been shown to be accurate in detailed molecular dynamics simulations of specific electron transfer reactions, such as the charge exchange reactions of aqueous ferric ions, and the primary electron transfer process in photosynthetic reactions centers.[18(a)–18(c)] It has also been quantitatively tested in voltage-dependent studies of transfer from metal electrodes to solvated molecular species.[18(d),18(e)] The harmonic approximation leads to a Gaussian transfer probability as a function of voltage, as experimentally observed.

If d_1 and d_2 are each 2 nm, $\lambda_{out}=400$ meV, about a factor of 20 larger than λ_{dp}. Figure 3 shows the vibrational configuration coordinate diagram for this case in water, as well as in vacuum. The water curve is shifted downward by $\sim$780 meV due to static dielectric solvation of the charged nanocrystal in water.[19] The activation energy G_{act} has increased to about 100 meV. In the presence of water, the dependence of the activation energy upon exothermicity is completely different than in vacuum. In the exactly symmetric case, the water polarization acts to ''self-trap'' the electron on the donor. The electron self-exchange rate is decreased by almost 10^2 by the water activation barrier.

In water the resonant nature of transfer to larger acceptors is completely lost, because of the ability of water polarization to accept the ΔG exothermicity. For exothermic 2- to 3-nm transfer in water (Fig. 5), G_{act} decreases and the transfer rate increases, as compared to resonant transfer.

By contrast, the configuration coordinate curves in vacuum for exothermic 2- to 3-nm transfer (Fig. 5) only cross far to the left, off the range of the figure. This creates a very high G_{act} and very slow rate. This situation is termed the ''Marcus inverted region'' in chemical electron transfer dynamics.

In heterogeneous p-Si, the local dielectric constant affects ΔG and λ, and hence k_{et}. An 80% porous sample in vacuum has a 1.64 average dielectric constant in effective medium theory,[20] close to the value in pure vacuum. Thus this simple model, a pair of nanocrystals in either water or vacuum, should apply to visibly emitting p-Si. Actually, the local variation about the effective medium dielectric constant can be large, on the order of 30% half width at half maximum.[21] This introduces another type of disorder into the electronic structure and kinetics, beyond nanocrystal size.

B. Electron-hole injection

In porous Si electroluminescent diodes, injected electrons and holes drift towards each other, and radiatively recombine in one nanocrystal. Consider two touching nanocrystals, one containing a hole and the other an electron. Considerable electrostatic free energy is released if one carrier injects into the other nanocrystal, as two initially charged nanocrystals convert into two neutral nanocrystals.

A related electrostatic problem is the nanocrystal donor binding energy G_B, defined as the polarization energy difference between an electron on an initially neutral nanocrystal, and on a nanocrystal containing an ionized fixed donor at $r=0$. If the electron charge distribution is $1S$ on both nanocrystals, then a fairly accurate analytical approximation is[8(d)]

$$G_B=-2e^2(1/\epsilon_{out}+1.44/\epsilon_{Si})/d. \tag{9}$$

This expression applies for a fixed positive charge at $r=0$ in the acceptor nanocrystal. Yet, G_B is not very sensitive to the donor position near $r=0$, and so G_B ought to be a fair approximation for the energy released when the electron jumps into a charged nanocrystal containing a $1S$ hole. For the case of two touching nanocrystals, G_B will be reduced by the nearest-neighbor Coulomb attraction energy, approximately $V_c=-e^2/\epsilon_{out}d_{12}$. In the general case with different size nanocrystals, the approximate free energy of electron-hole injection ΔG_{eh} is

$$\Delta G_{eh}=\Delta A(d_1)-\Delta A(d_2)+G_B(d_2)-V_c(d_{12}). \tag{10}$$

The λ_t of Sec. IV A is valid here. Figure 6 shows the calculated variation of the electron injection rate as a function of hole crystallite size, for a 2-nm nanocrystal donor. In vacuum, resonant $1S$-$1S$ injection for $d_1=d_2$ is suppressed because of an enormous ΔG_{eh}; for example, $\Delta G_{eh}=-1.03$ eV for 2-nm nanocrystals. $1S$-$2S$ injection is resonant for

2.1-nm acceptors, and $1S$-$3S$ for 4.5-nm acceptors. The $1S$-$2S$ near resonance for $d_1 \approx d_2$ is accidental, and would not occur for other donor sizes.

In water, the injection rate is very fast for all sizes; water has a huge enabling effect in electron-hole injection in small, just touching nanocrystals. This occurs for two reasons: ΔG_{eh} is smaller (-0.32 eV vs -1.03 eV for 2-nm size) and λ_t is larger than in vacuum.

C. Carrier trapping on surface states

Electrochemical synthesis of p-Si creates nearly complete H atom termination on nanocrystal surfaces. Total H atom termination should remove all surface states from within the nanocrystal band gap,[10(e)] and such crystallites should luminescence strongly. A small electron spin resonance (ESR) signal due to neutral dangling-bond surface states on Si atoms is present in freshly prepared p-Si.[22] Heating of p-Si to several hundred °C causes hydrogen gas evolution, an increase in the ESR signal, and a decrease in 23 C luminescence quantum yield. I now model the effect of a polar solvent on surface state trapping.

Consider one nanocrystal with an extra electron initially in a $1S$ orbital, and with one surface state. An electronic structure calculation by Hirao on $Si_{29}H_{36}$ nanocrystal shows that a neutral isolated dangling bond appears energetically in the middle of the nanocrystal band gap.[10(e)] Carrier trapping on such a localized state should lead to an additional local vibrational reorganization energy $\lambda_{ss} \sim 200$ meV, independent of size. The surface state trapping free energy in vacuum is

$$\Delta G_{ss} = \Delta A(d) - 550 \text{ meV} - \lambda_{ss}. \tag{11}$$

550 meV is the electronic trap depth below the bulk band edge. The total reorganization energy is $\lambda_{ss} + \lambda_{dp}$ in vacuum.

In water estimation of the change in ΔG_{ss} is uncertain, as a localized charge at the nanocrystal surface will have a field strong enough to cause dielectric saturation in water. Using an Eq. (1) type expression and size dependence, I estimate that ΔG_{ss} is increased by ~ 150 meV at 2-nm size. The water reorganization energy for a $1S$ electron coming from the interior towards the nanocrystal surface can be estimated from an expression of Kharkats, who considered reorganization energy for charge motion inside one spherical cavity in a polarizable fluid.[15(f)] If we consider transfer from the cavity center along a radius to point $r = 0.4d$, then

$$\lambda_K = (3.27e^2/d)(1/\epsilon_{op} - 1/\epsilon_s). \tag{12}$$

The total reorganization energy is $\lambda_K + \lambda_{dp} + \lambda_{ss}$.

Figure 7 shows the relative surface state trapping rates in vacuum, and in water. The rates in vacuum are quite slow because the trap depths are large, approaching 1 eV. In water the depths are even larger, but the rates increase by many orders of magnitude because of the large water reorganization energy. As in the electron hole injection case, the local presence of water completely dominates the kinetics.

V. DISCUSSION OF POROUS SILICON

A. Photoluminescence quenching by polar fluids

Three different groups report that the strong red photoluminescence of dry p-Si is quenched by reintroducing the

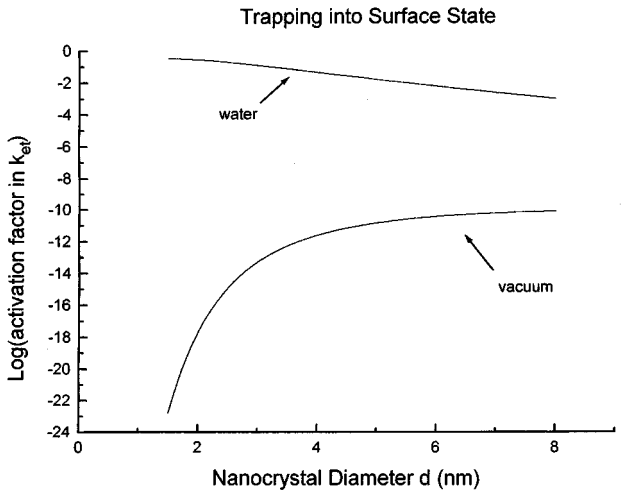

FIG. 7. Similar plot to Fig. 4, in this case for trapping of a carrier into a surface state, as a function of diameter.

p-Si film into aqueous electrolyte.[5] This quenching is entirely reversible: Li *et al.* cycled one sample out in and out of electrolyte more than 100 times. Dubin, Ozanam, and Chazalviel observed the same quenching, and additionally concluded that the quenching fluid must wet the Si-H terminated, internal pore surfaces.

Lauerhaas *et al.*[23] showed that polar organic molecules also reversibly quench the red luminescence, in both vapor and fluid forms.[22] The degree of quenching scales with the molecular dipole moment. Ben-Chlorin, Kux, and Schechter,[4] and Lauerhaas and Sailor[23] (LH), found methanol, which strongly wets a Si-H surface, to be an especially effective quencher in both the vapor and neat fluid forms. LH showed the quenching is *dynamic*: the lifetime shortens in the presence of methanol. This observation indicates that a polar environment increases the rate of a nonradiative process that competes with red photoluminescence.

The polar fluid quenching mechanism can be explained as trapping on a preexisting midgap surface state, as modeled in Sec. IV C. The ESR studies previously mentioned show that such deep traps are present in low concentration. Optically detected magnetic resonance experiments on the red emission show a signal due to dangling-bond resonances, indicating there is some kinetic communication between the red emitting state and the dangling bonds. The probability of a nanocrystal having one surface state might be expected to scale with d^2, and thus an increasingly polar environment should preferentially quench the larger, redder emitting nanocrystals. In some experiments, a weak greenish emission remains in aqueous electrolyte after the red emission is quenched. This may be photoluminescence of the smallest $\sim$1-nm nanocrystals that happen to have no surface states.

B. Carrier transport in wet and dry porous Si

The Sec. IV A model calculations show that the nature of p-Si transport changes from solid-state-like in vacuum, to proteinlike in water. In vacuum, p-Si behaves like a resonant tunneling device[24] in which carriers are very weakly coupled to the phonons. Resonant charge transfer occurs without activation barriers. Because of the high porosity, electrostatic

energies dominate crystallite energies. In water, the carriers are strongly coupled to polar fluid motions, and extremely exothermic processes occur rapidly without activation barriers. This often happens in sequential transfer of electrons among biological proteins, for example, in the photosynthetic reaction center.[18(d)] Electrostatic energies are partially screened. The Coulomb blockade transport characteristic of a single quantum dot in vacuum[24] is lost in water.

In order to discuss transport, consider a specific example: an 80% porous sample in electrical contact with the underlying Si wafer. As proposed by Vial and co-workers,[6(c)] and Lannoo and co-workers,[8(d),12] the film is charged by external bias so that the larger nanocrystals have one extra electron while the smaller ones remain neutral. All deep trap states are filled. Charge is compensated by flow of electrolyte ions (e.g., Na^+) into the film. In effect the Fermi level sits in the middle of the size disorder distribution. Consider also a film composed of 3-nm average size particles, with a distribution full width at half maximum (FWHM) 2–4 nm. If the touching particles form randomly connected paths, each nanocrystal touches 2–3 other nanocrystals.

At the Fermi level, the mobility is proportional to the hopping rate multiplied by the available density of states within kT energy. Hopping can only occur to touching nearest neighbors. This 2–4-nm size distribution has a free energy (ΔA) dispersion of 523 meV FWHM in vacuum, and 170 meV FWHM in water, as calculated from Eq. (1). Because the distribution is narrower in water, the density of states is about 3× higher.

If jumps occur to states within $kT=25$ meV at room temperature, however, then only nearly resonant jumps occur. This limits pathways if the donor has only 2–3 touching potential acceptors. For a 3-nm donor, rates in vacuum will be faster than in water for acceptors only in the narrow range $d_2=2.9$–3.2 nm. However, rates will be faster in water for $d_2>3.2$ nm and $d_2<2.9$ nm. For touching nanocrystals with FWHM 2–4 nm, it is likely that the fastest nearest-neighbor transfer process occurs in water. In vacuum, carriers will tend to be stationary on donors without suitable touching acceptors.

High porosity and wide particle dispersions favor faster transfer in water, while low porosity and narrower distributions favor faster transfer in vacuum. The microscopic pathways are different in water and in vacuum, for the same nanocrystal assembly. Exactly resonant pathways are favored in water, while alternating size pathways on the edge of the available thermal energy distribution are favored in water.

Experimentally, dry p-Si is extremely insulating. It shows an ac conductivity characteristic of activated hopping on a fractal network, with a wide range of activation energies.[25] A reversible conductivity increase of four orders of magnitude occurs upon exposure to methanol vapor.[4] There would appear to be at least two contributing mechanisms for this increase. First, as previously recognized, the free carrier concentration should increase as the donor binding energy decreases in polar solvent.[8] In vacuum, the donor binding energy is so high that very few free carriers exist. Second, the effective mobility should increase in a polar environment as discussed above.

C. Electroluminescence

The Sec. IV B calculation on electron injection into a nanocrystal containing a hole shows that water enhances the rate by orders of magnitude, and allows injection into nanocrystals of all sizes. The rates of other processes that dissipate energy, such as electron and hole injection into the porous layer from contacts, will also be enhanced. As a result, electroluminescent diode dynamics and efficiency should be strongly enhanced in electrolyte compared with vacuum, as experimentally observed. In the efficient liquid junction diodes, a carrier is injected from a solution redox molecule.[6] This type of exothermic injection is enhanced in water, just as injection from another nanocrystal.

The role of electrolyte permeation into p-Si is not simply to make efficient electrical contact inside the pores: if the liquid were poised at one electron chemical potential, then the p-Si layer would short out. However, electrolyte can facilitate the charging of the p-Si layer with carriers from the crystalline Si substrate, by compensating this charge with nonredox ions (e.g., Na^+) that flow into the wet p-Si from the bulk electrolyte. Such ions do not electrically dope the p-Si network. The ability of the wet p-Si to uniformly charge as voltage is applied is important in the proposed mechanism of voltage tunable color in electroluminescence.[6(c),6(d)]

VI. CONCLUSION AND FINAL COMMENTS

This paper shows how the classical theory of polar solvent involvement in electron transfer dynamics, developed originally for molecules and proteins, explains many observed differences between wet and dry p-Si at 23 C. This simple model is essentially without adjustible parameters. Two major aspects of the theory, the dielectric polarization treatment of the nanocrystal electron affinity, and the harmonic free-energy formula for the solvent coupling to the electron, have been previously verified.[11,18] The difference between wet and dry p-Si electrostatic energy levels was analyzed previously.[7,8]

In p-Si, electron-hole injection rates increase by orders of magnitude in the presence of polar solvent. This should also be true for net carrier mobilities, if the nanocrystal size distribution is wide and porosity is high. The quenching of red photoluminescence in wet p-Si at 23 C is assigned to trapping on midgap surface states. The rate of this process is slowed by many orders of magnitude in dry p-Si. Also, the presence of electrolyte in the pores facilitates the charging of the Si network with carriers of one sign in liquid junction electroluminescence.

Si nanostructures are remarkably sensitive to polar solvent because the intrinsic deformation potential coupling in covalent Si is so weak. As the electric field fringes out of the nanocrystal and interacts with the environment, the nanocrystal dynamics begin to behave like molecular dynamics. If there is no fringing, then hot carrier relaxation is expected to slow inside one quantum dot, when the energy differences between discrete excited states becomes larger than phonon energies.[26] This may occur for buried dots in epitaxial solid hosts, and for magnetically confined excitons in quantum wells. In nanocrystals, however, a new channel for ''electron-phonon'' coupling opens up via the fringing fields. Hot carrier relaxation for an electron or a hole in a Si nano-

structure should be faster in polar liquids than in vacuum. Even in a neutral exciton excited state, relaxation should increase as the field fringes locally outside the nanostructure.[7] Molecules might be viewed as extreme examples of quantum dots. Molecular excited-state relaxation rates are quite fast in almost all situations.

While Coulomb charging is incorporated, this model does not include the Coulomb gap predicted by Efros and Shklovskii for transport in disordered media.[27] Their Coulomb gap in the density of states results from electron-electron correlation at the Fermi Surface. In wet p-Si, screening will tend to decrease the importance of the Coulomb gap.

Recently, the consequences of solvent dielectric relaxation on p-Si carrier dynamics have also been qualitatively discussed from first principles by Chazalviel, Ozanam, and Dubin,[8(e)] however, with rather different conclusions.

ACKNOWLEDGMENTS

I enjoyed stimulating discussion and correspondence with D. Monroe, F. H. Stillinger, Al. L. Efros, N. Hill, and C. Delerue.

[1] Recent reviews and symposium proceedings: (a) Proceedings of the European Materials Research Society, Symposium F [Thin Solid Films **255**, Nos. 1 and 2 (1995)]; (b) *Microcrystalline and Nanocrystalline Semiconductors*, edited by R. W. Collins *et al.*, MRS Symposia Proceedings No. 358 (Materials Research Society, Pittsburgh, 1995); (c) *Porous Silicon Science and Technology*, edited by J. C. Vial and J. Derrien (Springer-Verlag, Berlin, 1995); (d) Light Emission from Novel Silicon Materials, edited by Y. Kanemitsu *et al.* [J. Phys. Soc. Jpn. **63** Suppl. B (1994)].

[2] K. Littau, P. Szajowski, A. Muller, A. Kortan, and L. Brus, J. Phys. Chem. **97**, 1224 (1993); W. Wilson, P. Szajowki, and L. Brus, Science **262**, 1242 (1993); S. Schuppler *et al.*, Phys. Rev. Lett. **72**, 2648 (1994); Phys. Rev. B **52**, 4910 (1995).

[3] L. Brus, P. Szajowski, W. Wilson, T. Harris, S. Schuppler, and P. Citrin, J. Am. Chem. Soc. **117**, 2915 (1995).

[4] M. Ben-Chorin, A. Kux, and I. Schechter, Appl. Phys. Lett. **64**, 481 (1994).

[5] K. Li, C. Tsai, J. Sarathy, and J. Campbell, Appl. Phys. Lett. **62**, 3192 (1993); V. Dubin, F. Ozanam, and J. Chazalviel, Phys. Rev. B **50**, 14 867 (1994); T. Ichinolhe, S. Nozaki, H. Ono, and H. Morisaki, Appl. Phys. Lett. **66**, 1644 (1995).

[6] (a) A. Halimaoui *et al.*, Appl. Phys. Lett. **59**, 304 (1991); (b) P. Bressers, J. Knapen, E. Meulenkamp, and J. Kelly, *ibid*. **61**, 108 (1992); (c) A. Bsiesy *et al.*, Phys. Rev. Lett. **71**, 637 (1993); (d) M. Ligeon *et al.*, J. Appl. Phys. **74**, 1265 (1993); (e) E. Kooij, R. Despo, and J. Kelly, Appl. Phys. Lett. **66**, 2552 (1995).

[7] L. Brus, J. Chem. Phys. **79**, 5566 (1983); **80**, 4403 (1984).

[8] (a) D. Babic, R. Tsu, and R. F. Greene, Phys. Rev. B **45**, 14 150 (1992); (b) R. Tsu and D. Babic, Appl. Phys. Lett. **64**, 1806 (1994); (c) C. Delerue, G. Allan, and M. Lannoo, Phys. Rev. B **48**, 11 024 (1993); (d) M. Lannoo, C. Delerue, and G. Allan, Phys. Rev. Lett. **74**, 3415 (1995); (e) J. Chazalviel, F. Ozanam, and V. Dubin, J. Phys. (France) I **4**, 1325 (1994).

[9] L. Wang and A. Zunger, Phys. Rev. Lett. **73**, 1039 (1994). See also Refs. 8(b) and 8(d).

[10] (a) B. Delley and E. Steigmeier, Phys. Rev. B **47**, 1397 (1993); (b) J. Proot, C. Delerue, and G. Allan, Appl. Phys. Lett. **61**, 1948 (1992); (c) L. Wang and A. Zunger, J. Chem. Phys. **100**, 2394 (1994); (d) N. Hill and B. Whaley, *Microcrystalline and Nanocrystalline Semiconductors* [Ref. 1(b)], p. 25; (e) N. Hill and B. Whaley, Phys. Rev. Lett. **75**, 1130 (1995); (f) T. Uda and M. Hirao, Light Emission from Novel Silicon Materials [Ref. 1(d)], p. 97.

[11] (a) S. Schmitt-Rink, D. Miller, and D. Chemla, Phys. Rev. B **35**, 8113 (1987); (b) B. K. Ridley, *Quantum Processes in Semiconductors*, 2nd ed. (Clarendon Press, Oxford, 1988), Eq. 6.112.

[12] E. Martin, C. Delerue, G. Allan, and M. Lannoo, Phys. Rev. B **50**, 18 258 (1994).

[13] (a) T. Holstein, Ann. Phys. **8**, 325 (1959); (b) C. Henry and D. Lang, Phys. Rev. B **15**, 989 (1977); (c) B. Ridley, J. Phys. C **11**, 2323 (1978); (d) for a tutorial see Ref. 11(b), Chap. 6.

[14] (a) D. Goguenheim and M. Lannoo, J. Appl. Phys. **68**, 1059 (1990); (b) Phys. Rev. B **44**, 1724 (1991).

[15] (a) R. Marcus, J. Chem. Phys. **24**, 966 (1956); (b) Faraday Discuss. Chem. Soc. **29**, 21 (1960); (c) V. Levich and R. Dogonadze, Dokl. Akad. Nauk. SSR **124**, 123 (1959); (d) J. Jortner, J. Chem. Phys. **64**, 4860 (1976); (e) for a review of dielectric continuum reorganization energy see E. German and A. Kuznetsov, Spectrochim. Acta **26**, 1595 (1981); (f) Yu. Kharkats, Elektrokhimiya **12**, 1866 (1976); (g) for a tutorial and analysis, see R. J. D. Miller *et al.*, *Surface Electron Transfer Processes* (VCH Publishers, New York, 1995), Chaps. 1 and 4; (h) for a review of molecular-dynamics applications see M. Newton and N. Sutin, Annu. Rev. Phys. Chem. **35**, 437 (1984).

[16] Nanocrystals have P,D, etc. excited states as well as S states. In the absence of detailed understanding of how the electronic coupling varies across all the excited acceptor states, I adopt the simplification of only considering excited S states. The resonant transfer spectrum in vacuum may be more dense than shown in Fig. 4.

[17] The saturation behavior of the water static dielectric constant is taken from Fig. 1.9 of J. O'M. Bockris and S. Khan, *Quantum Electrochemistry* (Plenum, New York, 1979).

[18] (a) R. Kuharski, J. Bader, D. Chandler, M. Sprik, M. Klein, and R. Impey, J. Chem. Phys. **89**, 3248 (1988); (b) J. Bader and D. Chandler, Chem. Phys. Lett. **157**, 501 (1989); (c) J. Bader, R. Kuharski, and D. Chandler, J. Chem. Phys. **93**, 230 (1990); (d) M. Marchi, J. Gehlen, D. Chandler, and M. Newton, J. Am. Chem. Soc. **115**, 4178 (1993); (e) C. J. Miller and M. Gratzel, J. Phys. Chem. **95**, 5225 (1991); (f) C. D. E. Chidsey, Science **251**, 919 (1991).

[19] Equations (2)–(4), which apply to an electron in a $1S$ orbital, have limited applicability to Si nanocrystals in water. For $\epsilon_{\text{out}}<11$, the polarization energy stabilizes the electron in the nanocrystal center, but for $\epsilon_{\text{out}}>11$, polarization stabilizes the electron on the surface. For small nanocrystals, KE(d) will dominate polarization energy, and the Sec. IV A analysis is valid. For large nanocrystals, the electron will come to the surface in some fashion. A crude estimate comparing the $1S$-$1P$ kinetic energy splitting to the polarization energy indicates the approximation should still be valid at $d=8$ nm. An accurate treatment would involve the frequency dependence and nonlin-

ear saturation of the water dielectric constant; it might best be done by molecular dynamics.
[20] Calculated using Eq. (4) of Y. H. Xie *et al.*, Phys. Rev. B **49**, 5386 (1994).
[21] P. Sheng and Z. Chen, Phys. Rev. Lett. **60**, 227 (1988).
[22] For an analysis see B. Meyer *et al.*, in *Microcrystalline and Nanocrystalline Semiconductors* [Ref. 1(b)], p. 454.
[23] J. Lauerhaas, G. Credo, J. Heinrich, and M. Sailor, J. Am. Chem. Soc. **114**, 1911 (1992); J. Lauerhaas and M. Sailor, Science **261**, 1567 (1993).
[24] For example, see M. Kastner, Rev. Mod. Phys. **64**, 849 (1992).
[25] M. Ben-Chorin, F. Moller, F. Koch, W. Schirmacher, and M. Eberhard, Phys. Rev. B **51**, 2199 (1995).
[26] H. Benisty, C. M. Sotomayor-Torres, and C. Weisbuch, Phys. Rev. B **44**, 10 945 (1991).
[27] A. L. Efros and B. Shklovskii, J. Phys. C **8**, L49 (1975).